

## Radiative Particle-in-Cell Simulations of Turbulent Comptonization in Magnetized Black-Hole Coronae

Daniel Grošelj<sup>1,2</sup>, Hayk Hakobyan<sup>3,4</sup>, Andrei M. Beloborodov<sup>5</sup>, Lorenzo Sironi<sup>2</sup>, and Alexander Philippov<sup>6</sup>

<sup>1</sup>Centre for mathematical Plasma Astrophysics, Department of Mathematics, KU Leuven, B-3001 Leuven, Belgium

<sup>2</sup>Department of Astronomy and Columbia Astrophysics Laboratory, Columbia University, New York, New York 10027, USA

<sup>3</sup>Computational Sciences Department, Princeton Plasma Physics Laboratory, Princeton, New Jersey 08540, USA

<sup>4</sup>Department of Physics and Columbia Astrophysics Laboratory, Columbia University, New York, New York 10027, USA

<sup>5</sup>Max Planck Institute for Astrophysics, D-85741 Garching, Germany

<sup>6</sup>Department of Physics, University of Maryland, College Park, Maryland 20742, USA

 (Received 26 January 2023; revised 30 September 2023; accepted 24 January 2024; published 23 February 2024)

We report results from the first radiative particle-in-cell simulations of strong Alfvénic turbulence in plasmas of moderate optical depth. The simulations are performed in a local 3D periodic box and self-consistently follow the evolution of radiation as it interacts with a turbulent electron-positron plasma via Compton scattering. We focus on the conditions expected in magnetized coronae of accreting black holes and obtain an emission spectrum consistent with the observed hard state of Cyg X-1. Most of the turbulence power is transferred directly to the photons via bulk Comptonization, shaping the peak of the emission around 100 keV. The rest is released into nonthermal particles, which generate the MeV spectral tail. The method presented here shows promising potential for *ab initio* modeling of various astrophysical sources and opens a window into a new regime of kinetic plasma turbulence.

DOI: [10.1103/PhysRevLett.132.085202](https://doi.org/10.1103/PhysRevLett.132.085202)

**Introduction.**—Luminous accreting black holes at the cores of active galaxies and in x-ray binaries are some of the most prominent examples of high-energy electromagnetic emission [1,2]. A particularly well-studied source is the binary Cyg X-1 [3], one of the brightest persistent sources of hard x rays in the sky. The emission spectra of x-ray binaries are routinely observed in the soft and hard states [4], with peak energies near 1 and 100 keV, respectively. The hard state is believed to originate from a hot “corona” of moderate optical depth [5,6], where the electrons Comptonize soft seed photons to produce the observed emission. The coronal electrons lose energy through inverse-Compton scattering, and therefore an energization process is needed in order to balance the electron cooling. The nature of this process is unknown [7]. In a number of proposed scenarios the electrons draw energy from magnetic fields. The released magnetic energy is then channeled into bulk flows, nonthermal particles, and heat [8–20].

A fraction of the electron kinetic energy in black-hole coronae is likely contained in nonthermal particles [7,21–23], which calls for a kinetic plasma treatment of their energization. Among the various pathways leading to particle energization, not only in black-hole accretion flows but in relativistic plasmas in general, turbulence has emerged as a prime candidate because it develops rather generically whenever the driving scale of the flow is much greater than the plasma microscales [24,25]. Recent kinetic simulations explored relativistic turbulence

in moderately [26–29] and strongly magnetized [30–35] nonradiative plasmas, and turbulent plasmas with a radiation reaction force on particles representing synchrotron or inverse-Compton cooling of optically thin sources [36–39]. However, existing simulations do not apply to turbulence in black-hole coronae, which have moderate optical depths.

In this Letter, we perform the first radiative kinetic simulations of turbulence in plasmas of *moderate optical depth* and demonstrate that our method can directly predict the observed emission from a high-energy astrophysical source. As an example, we investigate here the hard state of the archetypal source Cyg X-1. In the future, similar methods could be applied to study a variety of high-energy astrophysical systems.

**Method.**—We perform 3D simulations of driven turbulence using the particle-in-cell (PIC) code Tristan-MP v2 [40]. All simulations employ for simplicity an electron-positron pair composition. The PIC algorithm is coupled with radiative transfer accounting for the injection of seed photons, photon escape, and Compton scattering. The latter is resolved on a spatial grid composed of “collision cells” and incorporates Klein-Nishina cross sections [41,42]. The computational electrons (or positrons) and photons in a given collision cell are scattered using a Monte Carlo approach similar to [43,44], apart from a few technical adjustments described in Supplemental Material [45]. While the Compton scattering is modeled from first principles, we adopt for simplicity a more heuristic

approach for photon injection and escape, as discussed below.

The simulation domain is a periodic cube of size  $L$ . A mean magnetic field  $\mathbf{B}_0$  is imposed in the  $z$  direction. We achieve a turbulent state by continuously driving an external current in the form of a ‘‘Langevin antenna’’ [65] that excites strong Alfvénic perturbations on the box scale [26,66]. The box is initially filled with photons and charged particles in thermal equilibrium at temperature  $T_0$ . Given the lack of physical boundaries in the periodic box, we implement a spatial photon escape by keeping track of how each photon diffuses from its initial injection location. A given photon is removed from the box when it diffuses over a distance  $l_{\text{esc}} = L/2$  in any of the three Cartesian directions, so as to mimic escape from an open cube of linear size  $L$ . Each escaping photon is immediately replaced with a new seed photon, inserted at the location of the old particle, so that the total number of photons in the box remains constant. The momenta of injected seed photons are sampled from an isotropic Planck spectrum at the fixed temperature  $T_0$ .

Our setup has three key parameters: the pair plasma magnetization  $\sigma_e \equiv B_0^2/4\pi n_{e0}m_e c^2$ , the ratio  $n_{\text{ph0}}/n_{e0}$ , and the Thomson optical depth  $\tau_T \equiv \sigma_T n_{e0} l_{\text{esc}}$ , where  $n_{e0}$  is the mean density of electrons and positrons,  $n_{\text{ph0}}$  is the mean (x-ray and gamma-ray) photon density, and  $\sigma_T$  is the Thomson cross section. Our fiducial simulation has  $\sigma_e = 2.5$ ,  $n_{\text{ph0}}/n_{e0} = 250$ , and  $\tau_T = 1.7$ . The choice of  $\sigma_e$  and  $\tau_T$  mimics the conditions expected in black-hole coronae, which are believed to be strongly magnetized ( $\sigma_e \gtrsim 1$ ) and optically moderately thick ( $\tau_T \sim 1$ ) [6,67], whereas  $n_{\text{ph0}}/n_{e0}$  is chosen so as to achieve an amplification factor  $A \sim 10$  [defined below; see Eq. (1)], consistent with observations of hard states in x-ray binaries [7,68].

Other parameters are chosen as follows. The temperature of the seed photons is  $T_0/m_e c^2 = 10^{-3}$ . We set the frequency and decorrelation rate of the Langevin antenna [65] to  $\omega_0 = 0.9(2\pi v_A/L)$  and  $\gamma_0 = 0.5\omega_0$ , respectively, where  $v_A$  is the Alfvén speed. We define  $v_A = c[\sigma_e/(1 + \sigma_e)]^{1/2}$ . The chosen strength of the antenna current results in a typical amplitude  $\delta B \sim B_0$  for the large-scale fluctuating magnetic field. The simulation domain is resolved with  $1280^3$  cells for the PIC scheme and  $128^3$  collision cells for the Compton scattering. The size of the box is  $L/d_{e0} = 640$ , where  $d_{e0} = (m_e c^2/4\pi n_{e0} e^2)^{1/2}$  is the pair plasma skin depth. The time step for the PIC scheme and for Compton scattering is  $\Delta t = 0.45\Delta x/c$ , where  $\Delta x$  is the cell size of the PIC grid. The plasma and radiation are each represented on average with eight macroparticles per cell of the PIC grid. Additional simulations, numerical details, and discussions are included in Supplemental Material [45].

*Energy budget.*—Let us consider the energetics of the turbulent cascade. In steady state, the energy carried away by escaping radiation is balanced by the turbulence cascade

power (cf. [25,69]):  $n_{\text{ph0}}(\bar{E}_{\text{esc}} - \bar{E}_0)/t_{\text{esc}} \simeq \delta B^2/4\pi t_0$ , where  $\bar{E}_{\text{esc}}$  and  $\bar{E}_0$  are the mean energies of escaping and injected photons, respectively,  $t_{\text{esc}} = (\tau_T + 1)l_{\text{esc}}/c$  is the photon escape time associated with diffusion over scale  $l_{\text{esc}}$ , and  $t_0 = l_0/\delta v$  is the eddy turnover time at the turbulence integral scale  $l_0$  with velocity fluctuation  $\delta v$ . Using  $\delta v \simeq (\delta B/B_0)v_A$ , we then obtain

$$A \simeq 1 + \sigma_e(\tau_T + 1) \left(\frac{\bar{E}_0}{m_e c^2}\right)^{-1} \left(\frac{n_{e0}}{n_{\text{ph0}}}\right) \left(\frac{v_A}{c}\right) \left(\frac{\delta B}{B_0}\right)^3 \left(\frac{l_{\text{esc}}}{l_0}\right), \quad (1)$$

where  $A \equiv \bar{E}_{\text{esc}}/\bar{E}_0$  is the amplification factor. An effective electron temperature  $\Theta_{\text{eff}}$  can be obtained by balancing the radiative cooling rate  $\dot{U}_{\text{IC}}$  with the power carried away by the escaping photons. To estimate  $\dot{U}_{\text{IC}}$  we assume for simplicity that the radiation field is isotropic, which is well satisfied when  $\tau_T \ll 1$ ; for  $\tau_T \sim 1$  moderate anisotropies may arise due to the scattering of photons by the large-scale bulk motions [70]. In the regime of unsaturated Comptonization, relevant to black-hole coronae [71], we then have  $\dot{U}_{\text{IC}} \simeq 4f_{\text{KN}}\tau_T n_{\text{ph0}}\bar{E}_{\text{ph}}\Theta_{\text{eff}}c/l_{\text{esc}}$  (cf. [69]), where  $\Theta_{\text{eff}} \equiv \bar{u}^2/3$ ,  $u = \gamma\beta$  is the particle four-velocity in units of  $c$ ,  $f_{\text{KN}}$  is a Klein-Nishina correction factor [72], and  $\bar{E}_{\text{ph}}$  is the mean energy of a photon within the turbulent domain. Balancing  $\dot{U}_{\text{IC}}$  with  $n_{\text{ph0}}\bar{E}_{\text{esc}}/t_{\text{esc}}$  gives

$$\Theta_{\text{eff}} \simeq \frac{\bar{E}_{\text{esc}}}{4\bar{E}_{\text{ph}}f_{\text{KN}}\tau_T(\tau_T + 1)}. \quad (2)$$

$\Theta_{\text{eff}}$  is not to be confused with the proper plasma temperature. Rather, it should be regarded as a measure for the particle mean square four-velocity, which can include contributions from thermal, nonthermal, or bulk motions. For the timescale  $t_{\text{IC}} \simeq n_{e0}\bar{E}_e/(n_{\text{ph0}}\bar{E}_{\text{esc}}/t_{\text{esc}})$ , on which the electron kinetic energy is passed to the radiation, we find  $t_{\text{IC}}/t_0 \simeq (\bar{E}_e/m_e c^2)[\sigma_e(\delta B/B_0)^2]^{-1}$ , where  $\bar{E}_e$  is the mean kinetic energy per electron. Finally, the radiative compactness [6,73] can be expressed as  $\ell \simeq 4\tau_T\sigma_e(\delta B/B_0)^3(v_A/c)(l_{\text{esc}}/l_0)$  [45].

Figure 1 demonstrates the approach to a statistically steady turbulent state in our fiducial PIC simulation. The charged particles and photons are energized by the turbulent cascade, reaching a quasisteady state in roughly three light-crossing times  $L/c$  [74]. Unless stated otherwise, the various statistical averages reported below represent the mean values over the quasisteady state starting at  $tc/L \approx 3$  and extending until the end of the simulation. The fully developed turbulent state exhibits random ‘‘flaring’’ activity associated with the buildup and release of magnetic energy [Fig. 1(c)]. The system is radiation-dominated and strongly magnetized in the sense that both the box-averaged photon energy density  $\langle U_{\text{ph}} \rangle = n_{\text{ph0}}\bar{E}_{\text{ph}}$

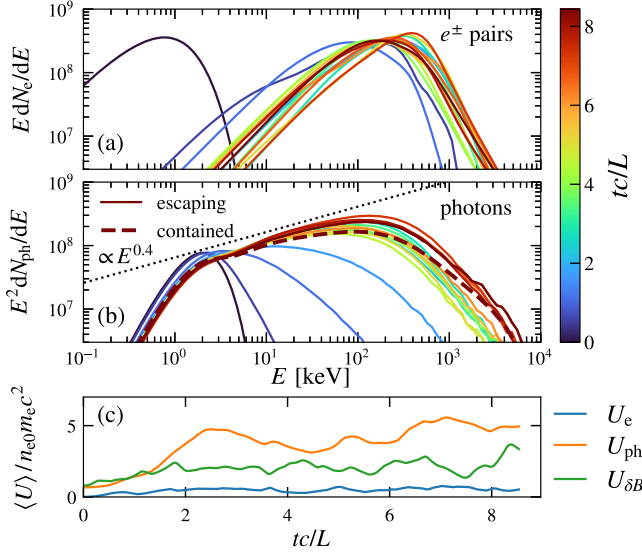


FIG. 1. Time evolution of the electron-positron (a) and escaping photon (b) energy spectrum, and the evolution of the box-averaged plasma, radiation, and magnetic energy density (c). Different colors in panels (a) and (b) represent the simulation time. Also shown is the spectrum of photons contained in the domain at the end of the simulation [dashed red curve in panel (b)].

and the fluctuating magnetic energy density  $\langle U_{\delta B} \rangle = \langle \delta B^2 \rangle / 8\pi$  exceed the average kinetic energy density  $\langle U_e \rangle = n_{e0} \bar{E}_e$  of pairs.

Consistent with observations [7], the escaping radiation spectrum exhibits in the statistically steady state a photon index close to  $\Gamma \approx 1.6$  between the photon injection energy of roughly 1 keV and the peak near 100 keV (corresponding to  $E^2 dN_{\text{ph}}/dE \propto E^{-\Gamma+2} \sim E^{0.4}$  in Fig. 1(b)). For our simulation parameters with  $\bar{E}_0/m_e c^2 \approx 2.7 \times 10^{-3}$ ,  $\delta B/B_0 \approx 1$ , and  $l_{\text{esc}}/l_0 \approx 1.3$  [75], Eq. (1) gives  $A \approx 12$ , in reasonable agreement with the typical value  $A \approx 9$  measured in the simulation. The compactness  $\ell \approx 19$  [45], which is comparable to the typical value  $\ell \sim 50$  inferred for the hard state of Cyg X-1 [6]. The simulated compactness is too low for a self-consistent balance between pair creation and annihilation [45]. Thus, a pair plasma composition is assumed here for computational convenience only. That our model does not include heavier ions is an aspect worth considering when comparing our results to magnetohydrodynamic (MHD) simulations.

The pairs develop over time a nonthermal spectrum [Fig. 1(a)] with mean kinetic energy per particle  $\bar{E}_e/m_e c^2 \approx 0.5$ . The nonthermal tail ( $E_e \gtrsim 600$  keV) contains about 30% of the kinetic energy. The effective temperature is raised by particles from the nonthermal tail to  $\Theta_{\text{eff}} \approx 0.6$ . A thermal plasma with the same  $\bar{E}_e$  as measured in our simulation would have a proper temperature  $T_e/m_e c^2 \approx 0.3$ . For reference, Eq. (2) predicts  $\Theta_{\text{eff}} \approx 0.2$  for our measured  $\bar{E}_{\text{esc}}/\bar{E}_{\text{ph}} \approx 1.4$  and  $f_{\text{KN}} \approx 0.5$  [76].

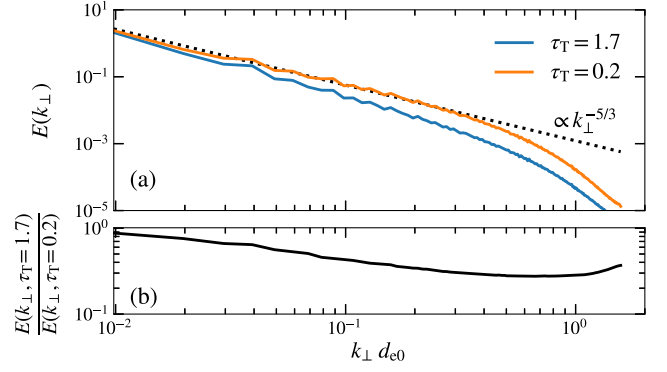


FIG. 2. 1D power spectra  $E(k_{\perp})$  of the turbulence energy as a function of the wave number  $k_{\perp}$  perpendicular to  $\mathbf{B}_0$  for  $\tau_T = 1.7$  and  $\tau_T = 0.2$  (a). Panel (b) shows the ratio of the turbulent spectra from the two simulations.

For the cooling timescale we find  $t_{\text{IC}}/t_0 \approx 0.2$ . Thus, the pairs pass their energy to the photons on a timescale shorter than the turbulent cascade time.

*Emission mechanism.*—The Comptonization of photons can occur through internal or bulk motions. In the fast cooling regime ( $t_{\text{IC}} < t_0$ ), a fraction  $f_{\text{bulk}}$  of the turbulence power is passed to the photons via bulk Comptonization *before* the cascade reaches the plasma microscales, leading to radiative damping of the turbulent flow [70,77,78]. This is demonstrated in Fig. 2, which shows the turbulence energy spectra  $E(k_{\perp})$ , defined as the sum of magnetic, electric, and bulk kinetic energy density spectra [79]. The spectrum  $E(k_{\perp})$  from our run with  $\tau_T = 1.7$  is compared against the result obtained from a simulation with  $\tau_T = 0.2$  but otherwise identical parameters. The spectra extend from the injection scale ( $k_{\perp} d_{e0} \sim 0.01$ ) into the kinetic range ( $k_{\perp} d_{e0} \gtrsim 1$ ), where the cascaded energy converts into plasma internal motions. Over the MHD range ( $k_{\perp} d_{e0} \ll 1$ ) the turbulence spectrum for  $\tau_T = 0.2$  exhibits a slope consistent with a classical cascade where  $E(k_{\perp}) \propto k_{\perp}^{-5/3}$  [80,81], while for  $\tau_T = 1.7$  the radiative damping becomes strong enough to steepen the spectrum [Fig. 2(a)]. This can be considered an example for how radiative effects render the turbulence spectra nonuniversal.

The steepening of the turbulence spectrum in our fiducial simulation with  $\tau_T = 1.7$  is related to the power lost via bulk Comptonization as follows. In the MHD range, it may be assumed that  $\Pi_{k_{\perp}} \sim \mathcal{F}_0 - \mathcal{D}_{k_{\perp}}^{\text{rad}}$ , where  $\Pi_{k_{\perp}}$  is the turbulent energy flux to perpendicular wave numbers larger than  $k_{\perp}$ ,  $\mathcal{F}_0$  is the external driving confined to the wave number  $k_0 \ll k_{\perp}$ , and  $\mathcal{D}_{k_{\perp}}^{\text{rad}}$  is the radiative dissipation rate between  $k_0$  and  $k_{\perp}$ . Since a fraction  $f_{\text{bulk}}$  of the cascade power is lost to radiation, we have  $\mathcal{D}_{k_{\perp}}^{\text{rad}} \sim f_{\text{bulk}} \mathcal{F}_0$ , and so  $\Pi_{k_{\perp}}/\Pi_0 \sim 1 - f_{\text{bulk}} \mathcal{D}_{k_{\perp}}^{\text{rad}}/\mathcal{D}_{k_{\perp}}^{\text{rad}}$ , where  $\Pi_0 \sim \mathcal{F}_0$  is the energy flux in the absence of damping. The flux can be approximated as  $\Pi_{k_{\perp}} \propto k_{\perp}^{2+\alpha} E(k_{\perp})^{1+\alpha}$ , with  $\alpha = 1/2$

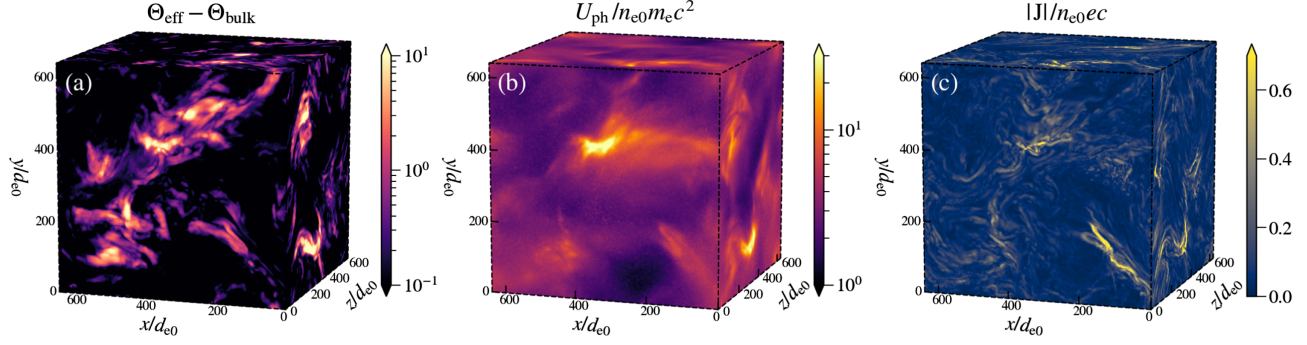


FIG. 3. Spatial structure of  $\Theta_{\text{eff}} - \Theta_{\text{bulk}}$  (a),  $U_{\text{ph}}$  (b), and  $|\mathbf{J}|$  (c), where  $\Theta_{\text{eff}}$  is the effective plasma temperature,  $\Theta_{\text{bulk}}$  is the “temperature” of turbulent bulk motions,  $U_{\text{ph}}$  is the photon energy density, and  $|\mathbf{J}|$  is the magnitude of the plasma electric current.

for the Goldreich-Sridhar turbulence model [80,81]. There follows the estimate

$$E(k_{\perp})/E_0(k_{\perp}) \sim (1 - f_{\text{bulk}} \mathcal{D}_{k_{\perp}}^{\text{rad}}/\mathcal{D}_{k_{\text{max}}}^{\text{rad}})^{\frac{1}{1+\alpha}}, \quad (3)$$

where  $E_0(k_{\perp})$  is the spectrum in the absence of significant damping. At the tail of the MHD range ( $k_{\perp} d_{e0} \sim 0.5$ ), we have  $f_{\text{bulk}} \sim 1 - [E(k_{\perp})/E_0(k_{\perp})]^{1+\alpha}$ , which can be taken as a proxy for measuring  $f_{\text{bulk}}$ . We substitute for  $E_0(k_{\perp})$  the spectrum obtained for  $\tau_T = 0.2$  and estimate from Fig. 2(b) that  $E(k_{\perp})/E_0(k_{\perp}) \approx 0.3$  near  $k_{\perp} d_{e0} \approx 0.5$  [82], indicating that roughly  $f_{\text{bulk}} \approx 80\%$  (using  $\alpha = 1/2$ ) of the total cascade power is passed to the photons via bulk Comptonization. The turbulent flow is dominated by motions transverse to the magnetic field [83], which renders the emission anisotropic. The intensity of Comptonized radiation escaping parallel to  $\mathbf{B}_0$  is about 3 times lower than the intensity emitted perpendicular to the mean magnetic field. Note that efficient bulk Comptonization is generally expected when the particles cool quickly ( $t_{\text{IC}} < t_0$ ). Guided by our simulation, we can give a simple estimate of  $f_{\text{bulk}}$  for  $t_{\text{IC}} < t_0$  as  $f_{\text{bulk}} \sim 1 - t_{\text{IC}}/t_0 \sim 1 - (\bar{E}_e/m_e c^2)[\sigma_e(\delta B/B_0)^2]^{-1}$ , which connects bulk Comptonization to the high- $\sigma_e$  regime.

Efficient bulk Comptonization implies that the plasma is essentially cold and its effective temperature is close to the “temperature” of turbulent bulk motions  $\Theta_{\text{bulk}} \equiv u_{\text{bulk}}^2/3$  [8], where  $u_{\text{bulk}}^2 = \beta_{\text{bulk}}^2/(1 - \beta_{\text{bulk}}^2)$  is the squared bulk four-velocity in units of  $c^2$ . In the simulation with  $\tau_T = 1.7$  we find on average  $\Theta_{\text{bulk}}/\Theta_{\text{eff}} \approx 50\%$ . In Fig. 3 we visualize the local difference  $\Theta_{\text{eff}} - \Theta_{\text{bulk}}$  at time  $tc/L = 6$  in our fiducial simulation. For reference, we also show the structure of the photon energy density and the magnitude of the plasma electric current. Over much of the volume the plasma is indeed cold, in the sense that at most locations the difference  $\Theta_{\text{eff}} - \Theta_{\text{bulk}}$  is very moderate. In a small fraction of the volume, typically near electric current sheets, the turbulent energy is intermittently released into internal motions, giving rise to “hot spots” with  $\Theta_{\text{eff}} - \Theta_{\text{bulk}} \gtrsim 1$ . The hot spot formation requires a rapid form of

energy release in order to outpace the fast cooling. One promising candidate is magnetic reconnection [45], which is known to promote particle energization magnetically dominated MHD [84–93] and kinetic [31,37,94–96] turbulent plasmas.

*Observational implications.*—Figure 4 shows the spectra from our fiducial PIC simulation, time-averaged over steady state, together with observations of Cyg X-1 in the hard state. The obtained emission spectrum closely resembles the observations. Differences between our simulation and observations are seen below 1 keV, where the observed spectrum is attenuated by absorption, between 10 keV and the peak, and around 1 MeV. We do not include the additional radiation component that is Compton-reflected from the disk [4], which affects the spectrum

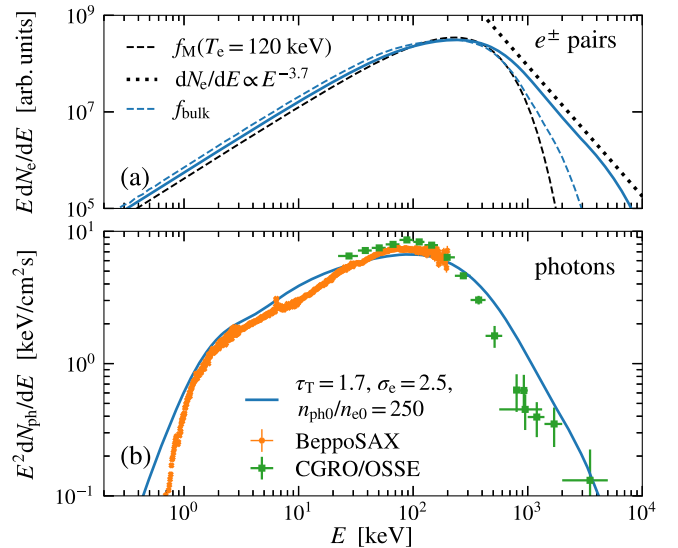


FIG. 4. Energy spectra of electron-positron pairs (a) and of the escaping radiation (b), overlotted with observations of the hard state in Cyg X-1 from BeppoSAX [99,100] and CGRO/OSSE [101]. The emission spectra are normalized with respect to OSSE. Dashed blue curve in panel (a) shows the energy distribution due to bulk motions alone. The dashed black curve shows a Maxwellian distribution fitted below 400 keV.

in the range between roughly 10 keV and the peak. Regarding the MeV tail, we note that the inclusion of synchrotron cooling [7] and pair creation [97,98] could soften the tail. Simulations with electron-ion compositions, pair creation and annihilation, and/or synchrotron emission can further constrain the physical conditions required to reproduce the observed MeV tail.

The strongly magnetized regime ( $\sigma_e \gtrsim 1$ ) explored here corresponds to a radiatively compact corona ( $\ell \gtrsim 10$ ) located roughly within 10 gravitational radii from the black hole [45]. A natural feature of our model is the formation of a nonthermal electron tail [Fig. 4(a)], which shapes the MeV emission. The distribution due to bulk motions alone [dashed blue curve in Fig. 4(a)] is significantly less nonthermal than the full distribution (solid blue curve), which implies that the nonthermal tail is mostly contributed by internal motions. We ran an additional simulation at  $\sigma_e = 0.1$  and found in comparison to our fiducial run a weaker nonthermal electron tail [45]. The results may also depend on the type of turbulence driving (e.g., the low-amplitude regime with  $\delta B \ll B_0$  is less favorable for the production of nonthermal particles [30,32,45]).

*Conclusions.*—We performed the first PIC simulations of plasma turbulence that self-consistently follow the evolution of radiation via Compton scattering. Our simulations focus on the conditions expected in magnetized coronae of accreting black holes [4,6], which have moderate optical depths and experience fast radiative cooling. Similar conditions can also arise in jets of gamma-ray bursts [70,77,78,102–104]. We obtain a spectrum of escaping x-rays similar to the observed hard-state spectrum of Cyg X-1, thus demonstrating that kinetic turbulence is a viable mechanism for the energization of electrons in black-hole coronae.

While the Compton scattering between the turbulent kinetic plasma and the radiation is treated self-consistently, we note that our present setup is still subject to a number of limitations. We do not model the emission of soft photons, pair creation, annihilation, or the global structure of the extended corona and the accretion disk. Instead, we adopt a local 3D periodic box approximation with a fixed average pair number density and with soft photon injection matching photon escape to sustain a fixed photon-to-electron ratio. A complete understanding of the x-ray emission from black-hole coronae may require a global kinetic model with detailed radiative transfer, which is presently lacking. Existing global models based on MHD simulations (e.g., [9–11]) suggest that the properties of the observed x rays depend not only on the mechanism of local energy release into radiation, but also on the geometric shape and multiphase structure of the corona.

In our local model, the emission is produced via Comptonization in a plasma energized by large-amplitude ( $\delta B \sim B_0$ ) Alfvénic turbulence. For a strongly magnetized plasma, we find that most of the turbulence power is directly

passed to the photons through bulk Comptonization. The rest is channeled into nonthermal particles at localized hot spots. For computational convenience, our simulations employ a pair plasma composition. The nature of turbulent Comptonization in electron-ion plasmas could differ from that in pair plasmas [45]. An important parameter is the fraction of turbulence power channeled into ion heating, which needs to be investigated with dedicated simulations. We also show that turbulent Comptonization manifests itself through nonuniversal turbulence spectra. As such, our simulations give a glimpse into a new regime of kinetic turbulence in radiative plasmas of moderate optical depth.

We acknowledge helpful discussions with L. Comisso, J. Nättilä, V. Zhdankin, B. Ripperda, and R. Mushotzky. We also thank N. Sridhar for his assistance in obtaining observational data for Cyg X-1. D.G. is supported by the Research Foundation—Flanders (FWO) Senior Postdoctoral Fellowship 12B1424N. D.G. was also partially supported by the U.S. DOE Fusion Energy Sciences Postdoctoral Research Program administered by ORISE for the DOE. ORISE is managed by ORAU under DOE Contract No. DE-SC0014664. All opinions expressed in this Letter are the authors’ and do not necessarily reflect the policies and views of DOE, ORAU, or ORISE. L.S. acknowledges support by the Cottrell Scholar Award. L.S. and D.G. were also supported by NASA ATP Grant No. 80NSSC20K0565. A.M.B. is supported by NSF Grants No. AST-1816484 and No. AST-2009453, NASA Grant No. 21-ATP21-0056, and Simons Foundation Grant No. 446228. A.P. was supported by NASA ATP Grant No. 80NSSC22K1054. The work was supported by a grant from the Simons Foundation (MP-SCMPS-00001470, to L.S. and A.P.). An award of computer time was provided by the INCITE program. This research used resources of the Argonne Leadership Computing Facility, which is a DOE Office of Science User Facility supported under Contract No. DE-AC02-06CH11357. Simulations were additionally performed on NASA Pleiades (GID s2754). This research was facilitated by the Multimessenger Plasma Physics Center (MPPC), NSF Grant No. PHY-2206607.

- 
- [1] R. A. Remillard and J. E. McClintock, *Annu. Rev. Astron. Astrophys.* **44**, 49 (2006).
  - [2] P. Padovani, D. M. Alexander, R. J. Assef, B. De Marco, P. Giommi, R. C. Hickox, G. T. Richards, V. Smolčić, E. Hatziminaoglou, V. Mainieri, and M. Salvato, *Astron. Astrophys. Rev.* **25**, 2 (2017).
  - [3] B. L. Webster and P. Murdin, *Nature (London)* **235**, 37 (1972).
  - [4] A. A. Zdziarski and M. Gierliński, *Prog. Theor. Phys. Suppl.* **155**, 99 (2004).
  - [5] F. Yuan and A. A. Zdziarski, *Mon. Not. R. Astron. Soc.* **354**, 953 (2004).

- [6] A. C. Fabian, A. Lohfink, E. Kara, M. L. Parker, R. Vasudevan, and C. S. Reynolds, *Mon. Not. R. Astron. Soc.* **451**, 4375 (2015).
- [7] J. Poutanen and A. Veledina, *Space Sci. Rev.* **183**, 61 (2014).
- [8] A. Socrates, S. W. Davis, and O. Blaes, *Astrophys. J.* **601**, 405 (2004).
- [9] J. D. Schnittman, J. H. Krolik, and S. C. Noble, *Astrophys. J.* **769**, 156 (2013).
- [10] Y.-F. Jiang, O. Blaes, J. M. Stone, and S. W. Davis, *Astrophys. J.* **885**, 144 (2019).
- [11] M. T. P. Liska, G. Musoke, A. Tchekhovskoy, O. Porth, and A. M. Beloborodov, *Astrophys. J. Lett.* **935**, L1 (2022).
- [12] L. H. S. Kadowaki, E. M. de Gouveia Dal Pino, and C. B. Singh, *Astrophys. J.* **802**, 113 (2015).
- [13] C. B. Singh, E. M. de Gouveia Dal Pino, and L. H. S. Kadowaki, *Astrophys. J. Lett.* **799**, L20 (2015).
- [14] B. Khiali, E. M. de Gouveia Dal Pino, and M. V. del Valle, *Mon. Not. R. Astron. Soc.* **449**, 34 (2015).
- [15] J. Kaufman and O. M. Blaes, *Mon. Not. R. Astron. Soc.* **459**, 1790 (2016).
- [16] A. M. Beloborodov, *Astrophys. J.* **850**, 141 (2017).
- [17] L. Sironi and A. M. Beloborodov, *Astrophys. J.* **899**, 52 (2020).
- [18] N. Sridhar, L. Sironi, and A. M. Beloborodov, *Mon. Not. R. Astron. Soc.* **507**, 5625 (2021).
- [19] J. M. Mehlhaff, G. R. Werner, D. A. Uzdensky, and M. C. Begelman, *Mon. Not. R. Astron. Soc.* **508**, 4532 (2021).
- [20] N. Sridhar, L. Sironi, and A. M. Beloborodov, *Mon. Not. R. Astron. Soc.* **518**, 1301 (2023).
- [21] G. Ghisellini, F. Haardt, and A. C. Fabian, *Mon. Not. R. Astron. Soc.* **263**, L9 (1993).
- [22] A. A. Zdziarski, A. P. Lightman, and A. Maciolek-Niedzwiecki, *Astrophys. J. Lett.* **414**, L93 (1993).
- [23] A. C. Fabian, A. Lohfink, R. Belmont, J. Malzac, and P. Coppi, *Mon. Not. R. Astron. Soc.* **467**, 2566 (2017).
- [24] V. Petrosian, *Space Sci. Rev.* **173**, 535 (2012).
- [25] D. A. Uzdensky, *Mon. Not. R. Astron. Soc.* **477**, 2849 (2018).
- [26] V. Zhdankin, G. R. Werner, D. A. Uzdensky, and M. C. Begelman, *Phys. Rev. Lett.* **118**, 055103 (2017).
- [27] V. Zhdankin, D. A. Uzdensky, G. R. Werner, and M. C. Begelman, *Astrophys. J. Lett.* **867**, L18 (2018).
- [28] V. Zhdankin, D. A. Uzdensky, G. R. Werner, and M. C. Begelman, *Phys. Rev. Lett.* **122**, 055101 (2019).
- [29] K. Wong, V. Zhdankin, D. A. Uzdensky, G. R. Werner, and M. C. Begelman, *Astrophys. J. Lett.* **893**, L7 (2020).
- [30] L. Comisso and L. Sironi, *Phys. Rev. Lett.* **121**, 255101 (2018).
- [31] L. Comisso and L. Sironi, *Astrophys. J.* **886**, 122 (2019).
- [32] J. Nättilä and A. M. Beloborodov, *Phys. Rev. Lett.* **128**, 075101 (2022).
- [33] C. Vega, S. Boldyrev, V. Roytershteyn, and M. Medvedev, *Astrophys. J. Lett.* **924**, L19 (2022).
- [34] C. Vega, S. Boldyrev, and V. Roytershteyn, *Astrophys. J. Lett.* **931**, L10 (2022).
- [35] V. Bresci, M. Lemoine, L. Gremillet, L. Comisso, L. Sironi, and C. Demidem, *Phys. Rev. D* **106**, 023028 (2022).
- [36] V. Zhdankin, D. A. Uzdensky, G. R. Werner, and M. C. Begelman, *Mon. Not. R. Astron. Soc.* **493**, 603 (2020).
- [37] L. Comisso and L. Sironi, *Phys. Rev. Lett.* **127**, 255102 (2021).
- [38] V. Zhdankin, D. A. Uzdensky, and M. W. Kunz, *Astrophys. J.* **908**, 71 (2021).
- [39] J. Nättilä and A. M. Beloborodov, *Astrophys. J.* **921**, 87 (2021).
- [40] H. Hakobyan, A. Spitkovsky, A. Chernoglazov, A. Philippov, D. Grosej, and J. Mahlmann, Princeton University/tristan-mp-v2: v2.6, Zenodo (2023), [10.5281/zenodo.7566725](https://zenodo.org/record/7566725).
- [41] G. R. Blumenthal and R. J. Gould, *Rev. Mod. Phys.* **42**, 237 (1970).
- [42] G. B. Rybicki and A. P. Lightman, *Radiative Processes in Astrophysics* (John Wiley & Sons, New York, 1979).
- [43] T. Haugbølle, J. T. Frederiksen, and Å. Nordlund, *Phys. Plasmas* **20**, 062904 (2013).
- [44] F. Del Gaudio, T. Grismayer, R. A. Fonseca, and L. O. Silva, *J. Plasma Phys.* **86**, 905860516 (2020).
- [45] See Supplemental Material at <http://link.aps.org/supplemental/10.1103/PhysRevLett.132.085202>, which includes Refs. [46–64], for additional numerical details, simulation results, and discussions.
- [46] B. E. Stern, J. Poutanen, R. Svensson, M. Sikora, and M. C. Begelman, *Astrophys. J. Lett.* **449**, L13 (1995).
- [47] H. Politano, A. Pouquet, and P. L. Sulem, *Phys. Plasmas* **2**, 2931 (1995).
- [48] P. Dmitruk, W. H. Matthaeus, and N. Seenu, *Astrophys. J.* **617**, 667 (2004).
- [49] P. D. Mininni, A. G. Pouquet, and D. C. Montgomery, *Phys. Rev. Lett.* **97**, 244503 (2006).
- [50] Y. Sentoku and A. J. Kemp, *J. Comput. Phys.* **227**, 6846 (2008).
- [51] R. Santos-Lima, A. Lazarian, E. M. de Gouveia Dal Pino, and J. Cho, *Astrophys. J.* **714**, 442 (2010).
- [52] G. L. Eyink, A. Lazarian, and E. T. Vishniac, *Astrophys. J.* **743**, 51 (2011).
- [53] G. Kowal, A. Lazarian, E. T. Vishniac, and K. Otmianowska-Mazur, *Nonlinear Processes Geophys.* **19**, 297 (2012).
- [54] V. Zhdankin, D. A. Uzdensky, J. C. Perez, and S. Boldyrev, *Astrophys. J.* **771**, 124 (2013).
- [55] M. Vranic, T. Grismayer, J. L. Martins, R. A. Fonseca, and L. O. Silva, *Comput. Phys. Commun.* **191**, 65 (2015).
- [56] L. H. S. Kadowaki, E. M. De Gouveia Dal Pino, and J. M. Stone, *Astrophys. J.* **864**, 52 (2018).
- [57] J. C. Rodríguez-Ramírez, E. M. de Gouveia Dal Pino, and R. Alves Batista, *Astrophys. J.* **879**, 6 (2019).
- [58] Y. Kawazura, A. A. Schekochihin, M. Barnes, J. M. TenBarge, Y. Tong, K. G. Klein, and W. Dorland, *Phys. Rev. X* **10**, 041050 (2020).
- [59] A. Lazarian, G. L. Eyink, A. Jafari, G. Kowal, H. Li, S. Xu, and E. T. Vishniac, *Phys. Plasmas* **27**, 012305 (2020).
- [60] E. Sobacchi, J. Nättilä, and L. Sironi, *Mon. Not. R. Astron. Soc.* **503**, 688 (2021).

- [61] J. T. Hinkle and R. Mushotzky, *Mon. Not. R. Astron. Soc.* **506**, 4960 (2021).
- [62] V. Zhdankin, *Astrophys. J.* **922**, 172 (2021).
- [63] B. Ripperda, M. Liska, K. Chatterjee, G. Musoke, A. A. Philippov, S. B. Markoff, A. Tchekhovskoy, and Z. Younsi, *Astrophys. J. Lett.* **924**, L32 (2022).
- [64] H. Zhang, L. Sironi, D. Giannios, and M. Petropoulou, *Astrophys. J. Lett.* **956**, L36 (2023).
- [65] J. M. TenBarge, G. G. Howes, W. Dorland, and G. W. Hammett, *Comput. Phys. Commun.* **185**, 578 (2014).
- [66] D. Grošelj, C. H. K. Chen, A. Mallet, R. Samtaney, K. Schneider, and F. Jenko, *Phys. Rev. X* **9**, 031037 (2019).
- [67] A. Merloni and A. C. Fabian, *Mon. Not. R. Astron. Soc.* **321**, 549 (2001).
- [68] A. M. Beloborodov, in High Energy Processes in Accreting Black Holes, Astronomical Society of the Pacific Conference Series Vol. 161, edited by J. Poutanen and R. Svensson (Astronomical Society of the Pacific, San Francisco, 1999), p. 295 [arXiv:astro-ph/9901108].
- [69] A. M. Beloborodov, *Astrophys. J.* **921**, 92 (2021).
- [70] J. Zrake, A. M. Beloborodov, and C. Lundman, *Astrophys. J.* **885**, 30 (2019).
- [71] S. L. Shapiro, A. P. Lightman, and D. M. Eardley, *Astrophys. J.* **204**, 187 (1976).
- [72] R. Moderski, M. Sikora, P. S. Coppi, and F. Aharonian, *Mon. Not. R. Astron. Soc.* **363**, 954 (2005).
- [73] P. W. Guilbert, A. C. Fabian, and M. J. Rees, *Mon. Not. R. Astron. Soc.* **205**, 593 (1983).
- [74] We ran simulations in smaller boxes up to  $tc/L \approx 15$  and saw no signs of secular energy growth or decay beyond  $tc/L \approx 3$ . This supports our notion of a *statistically* steady state in the larger but shorter fiducial run.
- [75] We define  $l_0 = \pi(\int k_{\perp}^{-1} E_B(k_{\perp}) dk_{\perp}) / (\int E_B(k_{\perp}) dk_{\perp})$ , where  $E_B(k_{\perp})$  is the 1D magnetic spectrum for wave numbers perpendicular to  $\mathbf{B}_0$ .
- [76] We use  $f_{\text{KN}} \approx \langle U_{\text{ph}} \rangle^{-1} \int (1 + 4\bar{\gamma}\epsilon)^{-1.5} f_{\epsilon} d\epsilon$ , where  $f_{\epsilon}$  is the photon spectral energy density,  $\bar{\gamma} = \bar{E}_{\epsilon}/m_e c^2 + 1$ , and  $\epsilon = E_{\text{ph}}/m_e c^2$  [72].
- [77] C. Thompson, *Mon. Not. R. Astron. Soc.* **270**, 480 (1994).
- [78] C. Thompson, *Astrophys. J.* **651**, 333 (2006).
- [79] The kinetic energy density spectrum is obtained as the power spectrum of  $\mathbf{w} = [n_e m_e c^2 \gamma_{\text{bulk}}^2 / (\gamma_{\text{bulk}} + 1)]^{1/2} \boldsymbol{\beta}_{\text{bulk}}$ , such that  $|\mathbf{w}|^2 = (\gamma_{\text{bulk}} - 1) n_e m_e c^2$ .
- [80] P. Goldreich and S. Sridhar, *Astrophys. J.* **438**, 763 (1995).
- [81] C. Thompson and O. Blaes, *Phys. Rev. D* **57**, 3219 (1998).
- [82] Bulk Comptonization is a meaningful concept as long as the turbulence is fluidlike, which is marginally satisfied up to the transition into the kinetic range. Thus, we measure  $E(k_{\perp})/E_0(k_{\perp})$  just slightly below  $k_{\perp} d_{e0} \sim 1$ .
- [83] J. Cho and A. Lazarian, *Mon. Not. R. Astron. Soc.* **345**, 325 (2003).
- [84] A. Lazarian and E. T. Vishniac, *Astrophys. J.* **517**, 700 (1999).
- [85] E. M. de Gouveia dal Pino and A. Lazarian, *Astron. Astrophys.* **441**, 845 (2005).
- [86] G. Kowal, A. Lazarian, E. T. Vishniac, and K. Otmianowska-Mazur, *Astrophys. J.* **700**, 63 (2009).
- [87] G. Kowal, E. M. de Gouveia Dal Pino, and A. Lazarian, *Phys. Rev. Lett.* **108**, 241102 (2012).
- [88] A. Lazarian, L. Vlahos, G. Kowal, H. Yan, A. Beresnyak, and E. M. de Gouveia Dal Pino, *Space Sci. Rev.* **173**, 557 (2012).
- [89] G. Eyink, E. Vishniac, C. Lalescu, H. Aluie, K. Kanov, K. Bürger, R. Burns, C. Meneveau, and A. Szalay, *Nature (London)* **497**, 466 (2013).
- [90] E. M. de Gouveia Dal Pino and G. Kowal, in *Magnetic Fields in Diffuse Media*, Astrophysics and Space Science Library Vol. 407, edited by A. Lazarian, E. M. de Gouveia Dal Pino, and C. Melioli (Springer, Heidelberg, 2015), p. 373, 10.1007/978-3-662-44625-6\_13.
- [91] M. Takamoto, T. Inoue, and A. Lazarian, *Astrophys. J.* **815**, 16 (2015).
- [92] M. V. del Valle, E. M. de Gouveia Dal Pino, and G. Kowal, *Mon. Not. R. Astron. Soc.* **463**, 4331 (2016).
- [93] A. Beresnyak and H. Li, *Astrophys. J.* **819**, 90 (2016).
- [94] F. Guo, X. Li, W. Daughton, H. Li, P. Kilian, Y.-H. Liu, Q. Zhang, and H. Zhang, *Astrophys. J.* **919**, 111 (2021).
- [95] H. Zhang, L. Sironi, and D. Giannios, *Astrophys. J.* **922**, 261 (2021).
- [96] A. Chernoglazov, H. Hakobyan, and A. Philippov, *Astrophys. J.* **959**, 122 (2023).
- [97] R. Svensson, *Mon. Not. R. Astron. Soc.* **209**, 175 (1984).
- [98] R. Svensson, *Mon. Not. R. Astron. Soc.* **227**, 403 (1987).
- [99] T. Di Salvo, C. Done, P. T. Życki, L. Burderi, and N. R. Robba, *Astrophys. J.* **547**, 1024 (2001).
- [100] F. Frontera, E. Palazzi, A. A. Zdziarski, F. Haardt, G. C. Perola, L. Chiappetti, G. Cusumano, D. Dal Fiume, S. Del Sordo, M. Orlandini, A. N. Parmar, L. Piro, A. Santangelo, A. Segreto, A. Treves, and M. Trifoglio, *Astrophys. J.* **546**, 1027 (2001).
- [101] M. L. McConnell, A. A. Zdziarski, K. Bennett, H. Bloemen, W. Collmar, W. Hermsen, L. Kuiper, W. Paciesas, B. F. Philips, J. Poutanen, J. M. Ryan, V. Schönfelder, H. Steinle, and A. W. Strong, *Astrophys. J.* **572**, 984 (2002).
- [102] M. J. Rees and P. Mészáros, *Astrophys. J.* **628**, 847 (2005).
- [103] F. Ryde, A. Pe'er, T. Nymark, M. Axelsson, E. Moretti, C. Lundman, M. Battelino, E. Bissaldi, J. Chiang, M. S. Jackson, S. Larsson, F. Longo, S. McGlynn, and N. Omodei, *Mon. Not. R. Astron. Soc.* **415**, 3693 (2011).
- [104] A. M. Beloborodov and P. Mészáros, *Space Sci. Rev.* **207**, 87 (2017).